The Meteoritical Society

Meteoritics & Planetary Science 44, Nr 12, 1853–1861 (2009)
Abstract available online at http://meteoritics.org

OpenOrb: Open-source asteroid orbit computation software including statistical ranging

Mikael GRANVIK[1], Jenni VIRTANEN[2*], Dagmara OSZKIEWICZ[3], and Karri MUINONEN[4]

[1]Institute for Astronomy, University of Hawai'i, 2680 Woodlawn Drive, Honolulu, Hawai'i 96822, USA
[2]Finnish Geodetic Institute, P.O. Box 15, 02431 Masala, Finland
[3]Observatory, P.O. Box 14, 00014 University of Helsinki, Finland
[4]Observatory, P.O. Box 14, 00014 University of Helsinki, Finland
Finnish Geodetic Institute, P.O. Box 15, 02431 Masala, Finland
[*]Corresponding author. E-mail: mgranvik@ifa.hawaii.edu

(Submitted 18 December 2008, revision accepted 28 August 2009)

Abstract–We are making an open-source asteroid orbit computation software package called OpenOrb publicly available. OpenOrb is built on a well-established Bayesian inversion theory, which means that it is to a large part complementary to orbit-computation packages currently available. In particular, OpenOrb is the first package that contains tools for rigorously estimating the uncertainties resulting from the inverse problem of computing orbital elements using scarce astrometry. In addition to the well-known least-squares method, OpenOrb also contains both Monte-Carlo (MC) and Markov-Chain MC (MCMC; Oszkiewicz et al. [2009]) versions of the statistical ranging method. Ranging allows the user to obtain sampled, non-Gaussian orbital-element probability-density functions and is therefore optimized for cases where the amount of astrometry is scarce or spans a relatively short time interval. Ranging-based methods have successfully been applied to a variety of different problems such as rigorous ephemeris prediction, orbital element distribution studies for transneptunian objects, the computation of invariant collision probabilities between near-Earth objects and the Earth, detection of linkages between astrometric asteroid observations within an apparition as well as between apparitions, and in the rigorous analysis of the impact of orbital arc length and/or astrometric uncertainty on the uncertainty of the resulting orbits. Tools for making ephemeris predictions and for classifying objects based on their orbits are also available in OpenOrb. As an example, we use OpenOrb in the search for candidate retrograde and/or high-inclination objects similar to 2008 KV_{42} in the known population of transneptunian objects that have an observational time span shorter than 30 days.

INTRODUCTION

To date, asteroid-orbit-computation packages available to the public such as OrbFit[1] by Milani et al. (2007) have largely been based on the so-called geometric orbit computation philosophy. The geometric approach is manifested in the use of strong assumptions when estimating the orbital uncertainties. For example, the least-squares method assumes that the resulting orbital-element probability-density function (PDF) is Gaussian. Other examples are the various line-of-variation methods (see, e.g., Bowell et al. 1993; Muinonen 1996; Milani 1999) which assume that the uncertainty is predominantly constrained to a single dimension in the six-dimensional orbital element space and—although one dimension is treated properly—the uncertainty in the remaining dimensions is often assumed Gaussian (see, e.g., Milani 1999).

OpenOrb is built on the well-established Bayesian inversion theory (see, e.g., Lehtinen 1988), which means that it contains fully non-linear methods and is thus to a large part complementary to the geometric orbit computation packages. As for the inverse problem of obtaining orbital-element PDFs from input astrometry, OpenOrb contains the statistical ranging method (hereafter referred to as ranging; Virtanen et al. 2001; Muinonen et al. 2001; Virtanen 2005) and the least-squares method (see, e.g., Muinonen and Bowell 1993). Ranging is used to solve the orbital inverse problem of estimating the orbital-element PDFs based on input

[1]http://adams.dm.unipi.it/~orbmaint/orbfit/

astrometry and is, in particular, optimized for cases where the amount of astrometry is scarce or spans a relatively short time interval. Ranging-based methods have successfully been applied to a variety of different problems such as rigorous ephemeris prediction (Granvik et al. 2003), orbital-element-distribution studies for transneptunian objects (Virtanen et al. 2003; Virtanen et al. 2008), the computation of invariant collision probabilities between asteroids and the Earth (Virtanen and Muinonen 2006), detecting linkages between astrometric asteroid observations within an apparition (Granvik and Muinonen 2005) as well as between apparitions (Granvik and Muinonen 2008), and in the rigorous analysis of the impact of orbital arc length and/or astrometric uncertainty on the uncertainty of the resulting orbits (Virtanen et al. 2005).

In what follows, we will briefly review the theory of Bayesian inversion (Theory section), describe the numerical methods included in OpenOrb (Numerical Methods section), give an overview of the software package (Software section) and, finally, give a topical example of what can be accomplished with the OpenOrb package (Results section).

THEORY

In orbit computation, the general observation equation describes the relation between observed positions and computed positions:

$$\psi(\mathbf{t}) = \Psi(\mathbf{P}, \mathbf{t}, t_0) + \varepsilon + \nu \quad (1)$$

The vector ψ contains the observed positions which are typically given as Right Ascension (R.A.) and Declination (Dec.) pairs for the observation dates $\mathbf{t}$. $\mathbf{P}$ contains the six orbital elements—usually Keplerian or Cartesian elements—at a specified epoch t_0. The nonlinear function ψ ($\mathbf{P}$, $\mathbf{t}$, t_0) gives the light-time-corrected topocentric positions computed from the osculating orbital elements at epoch t_0 for the observation dates $\mathbf{t}$. ε and ν describe the random and systematic errors, respectively. For most modern applications, the systematic error is small enough to be incorporated into the typically much larger random error. In what follows, the systematic error is assumed negligible, that is, $\nu = 0$.

In Bayesian inverse theory (see, e.g., Lehtinen 1988, and references therein), the parameters to be estimated are treated as random variables and the complete solution to the inverse problem is contained in the parameters' posterior probability densities. The posterior distribution p_p is proportional to the prior (p_{pr}) and the observational error (p_ε) PDFs:

$$p_p(\mathbf{P}) = C p_{pr}(\mathbf{P}) p_\varepsilon(\Delta\psi(\mathbf{P})) \quad (2)$$

$C = \left(\int p(\mathbf{P}, \psi) d\mathbf{P}\right)^{-1}$ is the normalization constant, where the joint PDF is $p(\mathbf{P}, \psi) = p_{pr}(\mathbf{P}) p_\varepsilon(\Delta\psi(\mathbf{P}))$. Whereas p_ε is evaluated for the residuals between the observed positions and the computed positions (*O-C* residuals) $\Delta\psi(\mathbf{P})$ and is usually assumed to be Gaussian due to the central-limit theorem, Muinonen and Bowell (1993) experimented with non-Gaussian noise statistics. They concluded that a significant improvement in the results, outweighing the more cumbersome analysis, could not be obtained.

As it is desirable that, for example, the asteroid-Earth collision probability does not depend on the type of orbital elements used in the analysis, we secure the invariance of the orbital-element PDF p_p in transformations between different types of orbital elements (e.g., from Keplerian to Cartesian) using Jeffreys' prior PDF ($p_{pr,J}$) (Jeffreys 1946):

$$p_{pr,J}(\mathbf{P}) \propto \sqrt{det\ \Sigma^{-1}(\mathbf{P})},$$

$$\Sigma^{-1} = \Phi(\mathbf{P})^T \Lambda^{-1} \Phi(\mathbf{P}) \quad (3)$$

Here Σ^{-1} is the information matrix evaluated for the local orbital elements $\mathbf{P}$, Φ contains the partial derivatives of the observed coordinates (usually R.A. and Dec.) with respect to the orbital elements, and Λ is the covariance matrix for the observational errors. Finally, the posterior orbital-element PDF is given by

$$p_p(\mathbf{P}) \propto \sqrt{\det\ \Sigma^{-1}(\mathbf{P})} \exp\left[-\frac{1}{2}\chi^2(\mathbf{P})\right],$$

$$\chi^2(\mathbf{P}) = (\Delta\psi(\mathbf{P}))^T \Lambda^{-1} \Delta\psi(\mathbf{P}) \quad (4)$$

The posterior PDF p_p can also include an informative prior PDF $p_{pr,inf}$, which is included as a separate factor in Equation 4

$$p_p(\mathbf{P}) \propto p_{pr,inf}(\mathbf{P}) \sqrt{\det\ \Sigma^{-1}(\mathbf{P})} \exp\left[-\frac{1}{2}\chi^2(\mathbf{P})\right]. \quad (5)$$

The informative prior PDF can, for example, be used to set constraints on the posterior PDF (see, e.g., Virtanen et al. 2001; Granvik et al. 2003; Granvik and Muinonen 2008), or to combine inversion results obtained for different observation sets (an orbital-element PDF computed from radar observations as a prior PDF for the inverse problem of optical astrometry, or vice versa).

The orbital-element PDF p_p obtained can be transformed to the joint PDF of any other parameter set ($\mathbf{F}(\mathbf{P}) = (F_1(\mathbf{P}), \ldots, F_K(\mathbf{P}))^T$) by the following relation given in Muinonen and Bowell (1993):

$$p(\mathbf{F}) = \int d\mathbf{P} p_p(\mathbf{P}) \delta_D(F_1 - F_1(\mathbf{P})) \ldots \delta_D(F_K - F_K(\mathbf{P})) \quad (6)$$

where δ_D is Dirac's delta function. For example, Equation 6 can be used to transform the orbital-element PDF from one set of elements to another (e.g., from Keplerian elements to Cartesian elements), or to propagate the orbital-element PDF to the ephemeris PDF. In practice, the initial PDF is

multiplied by the determinant of the partial-derivatives matrix (that is, the Jacobian matrix) computed between the new parameters and the initial parameters.

NUMERICAL METHODS

The basic OpenOrb executable (oorb) contains methods for the inversion of astrometric measurements for the orbital-element PDF, for ephemeris prediction, for the classification of solar-system objects based on their osculating elements, and for the propagation of the osculating elements from one epoch to another.

The methods for the solution of the inverse problem can be divided into two groups—the non-linear sampling methods, such as Monte-Carlo (MC) ranging, and the linearized single-point methods (least-squares with linearized covariances; LSL). For a description of the latter see, for example, Virtanen et al. (2005).

Ranging maps the orbital-element PDF with a specified number of sample orbits. Each sample orbit is computed using the following scheme in MC ranging: Two observations are chosen from the data set and a random deviate is added to all four coordinates to mimic observational noise. Next, a random topocentric distance is drawn from a uniform distribution for the first observation date using a, typically, broad interval such as 0 AU to 100 AU. The topocentric distance for the second observation date is generated from an interval relative to the topocentric distance on the first observation date. Since the location of the observatory with respect to the Sun is usually known, the four plane-of-sky coordinates and the two topocentric distances can be transformed into two heliocentric positions corresponding to the two observation dates. An orbit can be computed using the two heliocentric positions by using, e.g., the so-called *p*-iteration method or the so-called continued-fraction method (Danby 1992). The generated sample orbit is then used to compute predicted positions for the other observation dates. If the *O*-*C* residuals are acceptable and the PDF value is good enough with respect to the until-then best-fit orbit (the so-called $\Delta\chi^2$ criterion), the sample orbit is accepted. The inversion can be sped up by iteratively adjusting the intervals for the topocentric distances either by performing the simulation for a smaller number of sample orbits before performing the full-scale inversion (Virtanen et al. 2003) or by starting with only two observations and adding more observations step by step (Granvik and Muinonen 2005). In addition to the MC ranging described above, the novel Markov-Chain MC ranging as described by Oszkiewicz et al. (2009) is also included in OpenOrb.

SOFTWARE

The core of the GPL-licensed OpenOrb package (http://code.google.com/p/oorb) is written in Fortran 90/95 using an object-oriented programming paradigm (Decyk et al. 1997). The package also contains Python wrappers for selected tasks deemed useful for the Large Synoptic Survey Telescope (LSST) and for the Panoramic Survey Telescope And Rapid Response System (Pan-STARRS).

The Fortran core is divided into main programs, classes, modules, and script files. Generic routines such as tools for statistics, random-number generation, numerical integration, linear algebra, and least-squares estimation are located in the modules, whereas tools specific for solar-system orbits—often building upon the routines in the modules—are found in the classes. The main programs make use of the classes for computations, modules for I/O, and Gnuplot scripts for plotting the results. The contents of selected classes are summarized in Table 1. Note that there is some overlap of the routines in the different classes since Fortran 90/95 does not support inheritance. It would be trivial, albeit laborious, to remove the overlaps by using the inheritance feature available in the Fortran 2003 standard. The main benefit of making the software object oriented is that it is straightforward to build main programs that make use of the classes, because one does not have to deal with details such as, for example, array sizes or I/O.

OpenOrb is accompanied by documentation such as instructions for installation and usage, but it is expected that the user is familiar with the theory behind state-of-the-art orbit computation methods as well as with the Bayesian approach, e.g., through published literature such as the references given below. If the user intends to publish results obtained with OpenOrb, we would encourage the user to contact MG or JV in case of any doubt regarding the procedures or interpretation of the results.

For the input and output of astrometric measurements, OpenOrb allows the user to choose between several formats such as, for example, the current Minor Planet Center (MPC) format and the Data Exchange Standard (DES; Milani et al. 2007) format to be used by Pan-STARRS. For the orbits, OpenOrb primarily uses its own format but the DES format is also supported. The computations can be done using either heliocentric Cartesian or Keplerian orbital elements and, in addition to these, the results can also be shown using, for example, cometary elements.

RESULTS

In what follows we will give a few examples of what OpenOrb can be used for. Gladman et al. (2009) reported the discovery of 2008 KV_{42}, the first retrograde transneptunian object (TNO). Using all 15 astrometric measurements available on 15 December 2008 and assuming an astrometric uncertainty of 0.3 arcseconds, we use OpenOrb to obtain an orbital-inclination (ι) estimate of $103.66^{+0.61}_{-1.02}$ degrees which agrees with MPC's solution (http://www.cfa.harvard.edu/mpec/K08/K08O02.html). The limits are equivalent to the 3σ

Table 1. Descriptions of selected classes in OpenOrb.

Class	Description of the data type	Selected capabilities
Time	Date	Conversions between different time scales (e.g., UTC, UT1, ET) and formats (e.g., modified Julian date, calendar date).
Spherical coordinates	6-vector containing the distance, longitude, latitude, and their time derivatives.	Rotations between ecliptic and equatorial coordinates, addition of Gaussian or uniform noise into coordinates.
Cartesian coordinates	6-vector containing the Cartesian position and velocity.	Rotations between Cartesian ecliptic and equatorial coordinate systems, transformation to/from spherical coordinates.
Observatory	Basic observatory data such as the IAU code, the geocentric coordinates, the name, etc.	Data storage only.
Observatories	List of observatory objects.	Input from observatory code file distributed by the Minor Planet Center. Computations of geocentric and heliocentric observatory coordinates as a function of time and observatory code.
Observation	Spherical 6-vector containing distance, longitude (R.A.), latitude (Dec.), and their time derivatives. Typically only R.A. and Dec. used.	Computation of the solar elongation.
Observations	A set of observation objects as typically found in a single file.	I/O of observations, sorting of observations, computation of observational time spans.
Orbit	A single 6-parameter orbit without uncertainty information.	Two-body and n-body propagation, solution of the two-point boundary-value problem, transformations between different orbital-element types, single-point ephemerides.
Stochastic orbit	A single 6-parameter orbital solution with uncertainty information given either as a sampled PDF or a least-squares solution accompanied by a covariance matrix.	MC and MCMC Ranging, LSL, ephemeris PDF, propagation of orbital-element PDF in time, object classification based on orbital-element PDF.

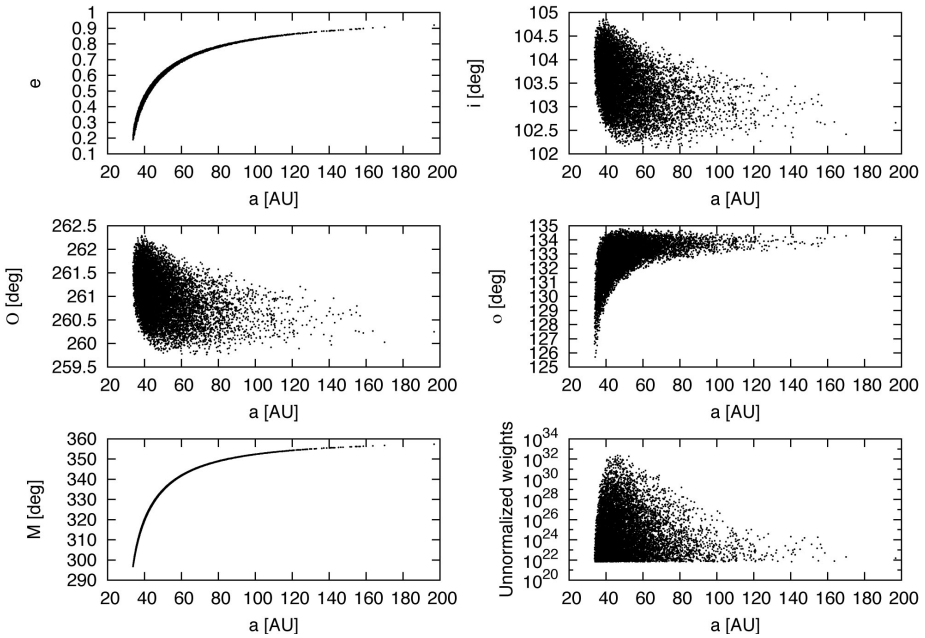

Fig. 1. Keplerian orbital-element PDF for the first verified retrograde TNO, 2008 KV_{42}, including all available data as of 15 December 2008. The observational time span is 37.8 days and the number of observations is 15. The two-body dynamical model was used due to the short observational time span.

limits of a one-dimensional Gaussian distribution, which means that they include 99.73002% of the probability mass. The plotted inclination distribution (Fig. 1) is wider than the given uncertainty limits, because we required a maximum $\Delta\chi^2 = 50$ between the maximum-likelihood (ML) orbit and the worst-fitting orbit which includes 99.99999953% of the total probability mass. Thus, even with an observational time span of only 38 days, the inclination of this TNO is extremely well determined.

To obtain the uncertainty estimate for the inclination we first sampled the Keplerian orbital-element PDF using MC ranging (Fig. 1). Then we normalized the sum of the sample

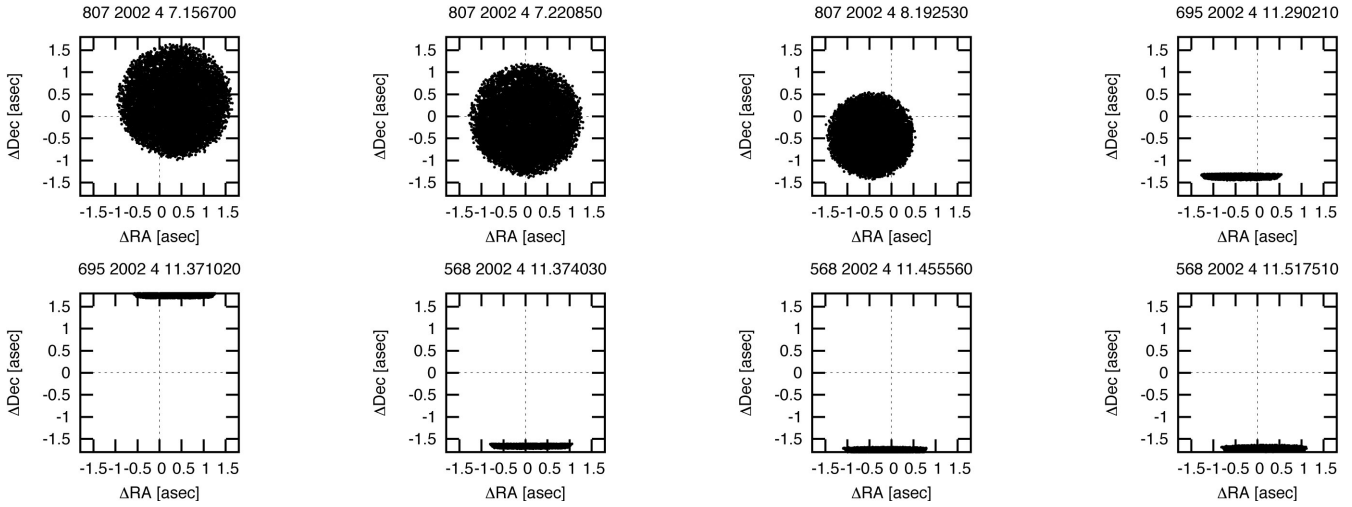

Fig. 2. Automatically generated residual stamps for 2002 GC_{32}. A possible outlier observation is suggested by the distorted distribution of *O-C* residuals, and the general trend points toward the observation obtained on 2002 April 11.371020 UTC (lower left panel) since it is the only cloud with a substantial positive offset in Dec.

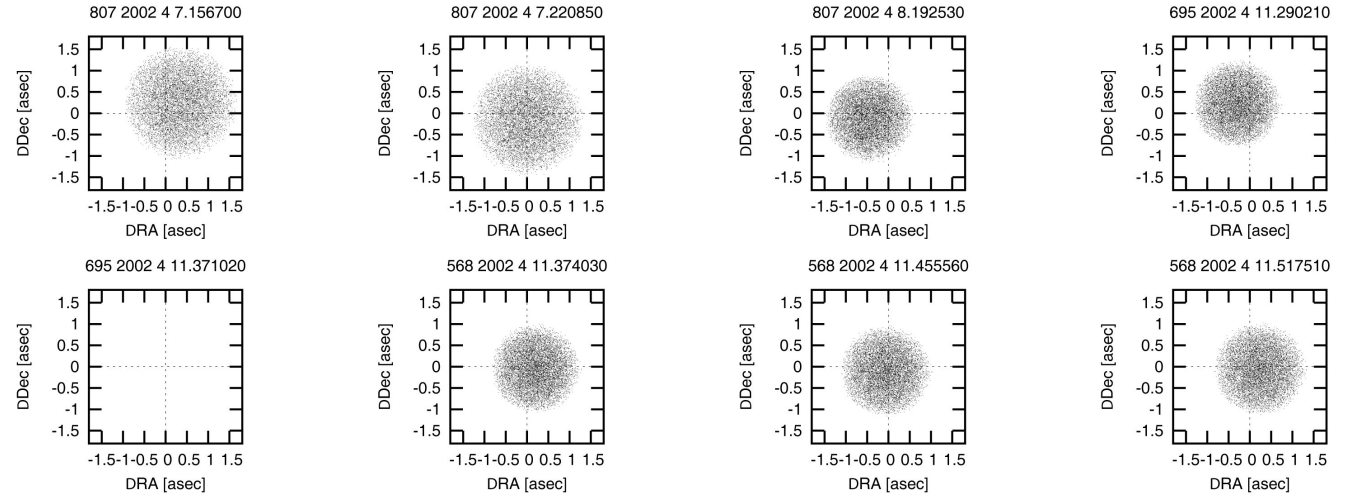

Fig. 3. Residual stamps after automatically discarding the outlier observation show an improved fit. With a mean residual of +3.4 arcseconds in Dec., the outlier observation is too far off to allow any part of the residual cloud to fall within the boundaries of the residual stamp.

orbits' relative weights to unity and computed the limits by starting from the ML orbit (the orbit with the largest relative weight) and going to smaller relative weights while recording the extrema of the inclination. When the sum of the relative weights of the orbits accounted for is larger than 0.9973002 we have obtained the 3σ-equivalent boundaries for the inclination.

When faced with a short observational time span (often about 24 hours) for a TNO, the MPC usually generates a "best-guess" orbit which is direct and as circular as possible. While this approach is useful in the sense that—based on cosmogonic assumptions—a TNO is more likely to have a direct orbit than a retrograde orbit, it begs the following question: have other TNOs been erroneously given direct orbits based on scarce data and single-point estimates combined with implicit assumptions? Note that Virtanen et al. (2008) have already suggested that other objects with retrograde orbits may well exist in the known TNO population.

We used a sample of 378 objects labeled TNOs (semimajor axis $a > 30$ AU) that have observational time spans less than 30 days and were discovered before 1 January 2009 (MPCORB.DAT dated July 30, 2009). First, we ran MC ranging on the 378 TNOs and obtained their Keplerian orbital-element PDFs assuming an astrometric uncertainty of 0.3 arcseconds. The so-called residual stamps are automatically generated when using the sampling methods. The stamps show the distributions of the residuals between the observed positions and positions predicted for the same dates. For some objects the residual stamps suggest

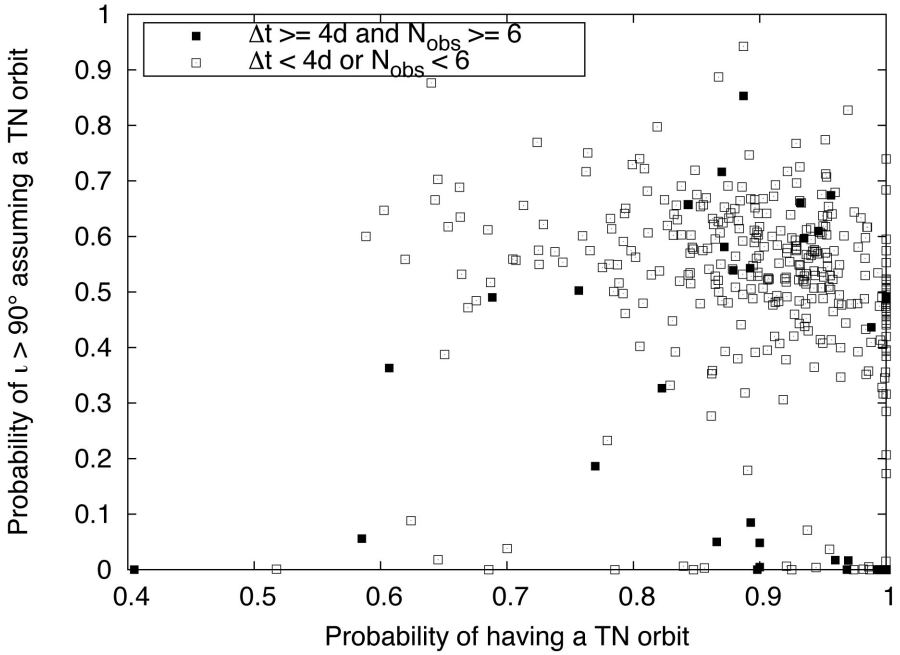

Fig. 4. The probability for $\iota > 90°$ when postulating a TN orbit plotted against the probability for a TN orbit for each of the selected 378 TNOs. The filled squares refer to objects more extensively observed than the unfilled squares. Interestingly, 2006 LM is outside of the boundaries of this plot since it has almost zero probability of being a TNO. Instead it has an almost 100% probability of being a retrograde main-belt object, which would make it the first in its class if verified.

Table 2. Candidate retrograde TNOs.

Designation	Δt[a]	N_{obs}[b]	P_{TN}[c]	P_{rTN}[d]	MLι[e]	1σ-equiv. ι[f]
1996 KY_1	8.14	8	0.89	0.54	122.18	21.45–138.95
1996 TC_{68}	6.10	6	0.88	0.54	147.04	17.14–157.41
2000 PQ_{30}	5.03	6	0.84	0.66	179.22	0.76–179.24
2000 QG_{226}	5.17	9	0.87	0.58	177.31	1.67–177.84
2000 QH_{226}	5.11	8	0.76	0.50	176.03	2.05–176.58
2000 QK_{226}	5.19	9	0.96	0.67	127.48	26.26–141.35
2001 FJ_{194}	9.15	11	0.89	0.85	159.38	13.19–163.34
2001 FN_{194}	9.14	9	0.87	0.72	163.29	8.84–167.58
2002 GC_{32}	4.36	8	0.93	0.66	176.78	2.49–176.94
2002 PR_{170}	29.78	8	0.95	0.61	178.85	0.84–178.93
2002 VC_{95}	18.11	11	0.94	0.60	177.00	2.34–177.44

[a]Observational time span in days.
[b]Number of observations available.
[c]Probability of having a TN orbit.
[d]Probability of $\iota > 90°$ when postulating a TN orbit.
[e]ML value for inclination in degrees.
[f]Inclination limits (in degrees) that include 68.3% of the total probability mass.

that outlier observations—that is, observations with anomalously large *O-C* residuals—are present. 2002 GC_{32} is a good example of an object with an outlier observation (Fig. 2); the single outlier distorts the whole solution in residual space. By automatically removing the fifth observation we get a better fit (Fig. 3). Note that for longer orbital arcs the use of the two-body dynamical model instead of the *n*-body dynamical model can lead to a high fraction of apparent outliers.

Next we computed the 3σ-equivalent boundaries for the inclination for all objects as was done for 2008 KV_{42} using a TNO a priori, that is, we only included sample orbits with $a > 30$ AU (hereafter referred to as transneptunian, or TN, orbits). Since it turns out that 351 of the 378 objects can have retrograde TN orbits, that is, $\iota > 90°$, based on the 3σ-equivalent limits, we need to reduce the number of candidates. To this end, we compute the probability for each object to have a TN orbit as well as the probability of $\iota > 90°$ when postulating a TN orbit (Fig. 4). Of the less scarcely observed objects, 11 have a greater than 75% probability of

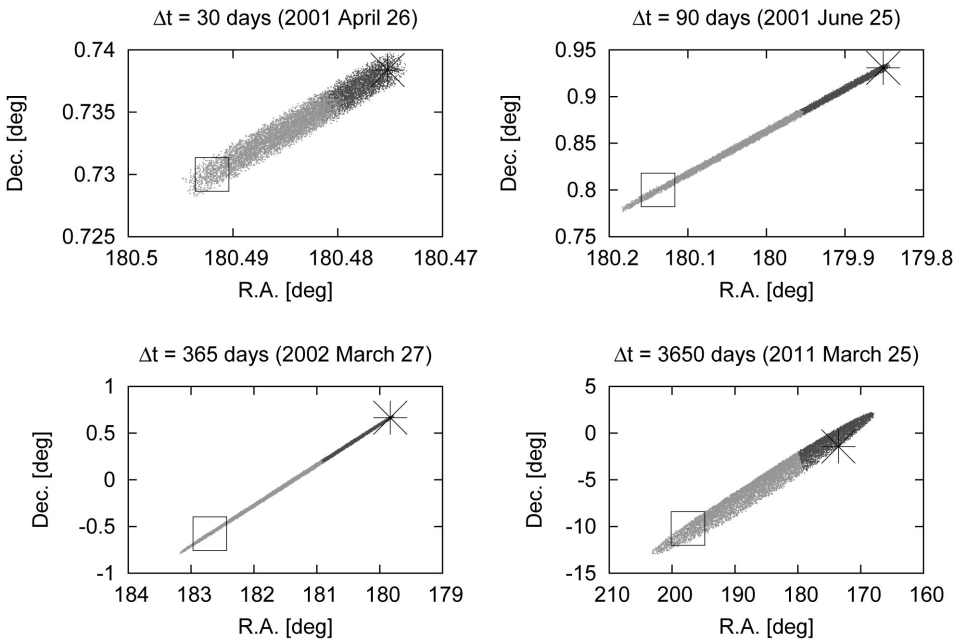

Fig. 5. Ephemeris predictions for 2001 FJ_{194} corresponding to the direct (light gray) and retrograde (dark gray) parts of the orbital-element PDF 30, 90, 365, and 3650 days after the last observation date. Note that the direct and retrograde solutions form two groups and the border between these groups becomes more obvious with time. The star symbol is the ML estimate, whereas the square is based on the orbit preferred by the MPC.

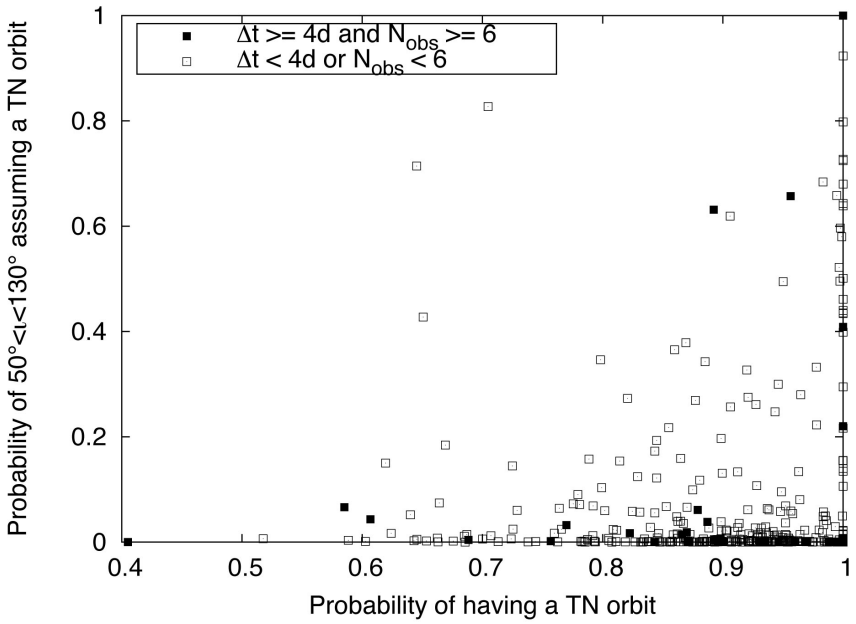

Fig. 6. The probability for 50°ι130° when postulating a TN orbit plotted against the probability for a TN orbit for each of the 378 selected TNOs. The filled squares refer to objects more extensively observed than the unfilled ones.

TN orbits and a greater than 50% probability of $\iota > 90°$ when postulating a TN orbit (Table 2).

So the question is why where these 11 objects not followed up until their orbital uncertainties would have been small enough to decide whether they are on direct or retrograde orbits? The possible answers are a lack of suitable telescope time or lack of interest due to unremarkable physical parameters. But assuming that someone has indeed tried to make follow-up observations of these objects without success, then what would a retrograde orbit imply for follow-up ephemerides? Figure 5 shows the ephemeris PDF separately for direct and retrograde orbits 30, 90, 365, and 3650 days after discovery for 2001 FJ_{194}, the object with the highest probability for a retrograde TN orbit from Table 2

Table 3. Candidate ι > 90° TNOs. Abbreviations are the same as those used in Table 2.

Designation	Δt	N_{obs}	P_{TN}	$P_{90°TN}$[a]	MLι	1σ-equiv. ι
1996 KY_1	8.14	8	0.89	0.63	122.18	21.45–138.95
2000 QK_{226}	5.19	9	0.96	0.66	127.48	26.26–141.35
2002 GM_{32}	4.41	5	0.65	0.71	121.38	28.25–136.63
2002 PZ_{152}	2.33	5	0.98	0.68	121.61	27.38–135.16
2004 DF_{77}	17.00	4	1.00	0.72	108.24	30.55–131.39
2004 TW_{357}	24.97	4	0.91	0.62	40.52	26.55–129.06
2007 DA_{61}	28.98	78	1.00	1.00	76.72	76.71–76.74

[a]Probability for 50°ι130° when postulating a TN orbit.

based on 11 observations on four different nights over a time span of 9.2 days. The ephemerides show that if the object has a retrograde orbit, it might now be lost. On the other hand, three months after its discovery, the total width of the ephemeris uncertainty region was still only about 20 minutes of arc. The relatively small uncertainty should thus have allowed a straightforward recovery of the object regardless of its inclination.

Gladman et al. (2009) put forward the idea that the reservoir supplying TNOs with inclinations around 90° is a hitherto unknown population. Based on their dynamical simulations, they claim that surveys should have found a larger fraction of the hypothetical population than is currently known—even after correcting for the strong observational biases. Figure 6 shows that several additional members of the hypothetical population may already have been detected, but the short observational time spans make it hard to draw any definite conclusions. Table 3 lists the objects that have a greater than 50% probability for 50°ι130° and an observational time span greater than two days.

Although the previous example deals with TNOs, OpenOrb is routinely used for other solar-system objects as well. The software is, for instance, used routinely in the Pan-STARRS Moving Object Processing System (MOPS) to compute near-Earth objects' Minimum Orbital Intersection Distances (MOIDs) with respect to the Earth's orbit, and it will also be used in the scientific analysis of other populations detected during the 3.5-year survey to be carried out with the Pan-STARRS' single-telescope prototype.

Acknowledgments–MG's work has been funded by a grant from the NASA NEOO program to R. Jedicke (NNX07AL28G) and grant #125335 from the Academy of Finland. J. V.'s work supported by a grant from the Väisälä fund. Research by DO supported by EU Marie Curie TMR project entitled "European Leadership in Space Astrometry" (ELSA). We want to thank Tim Spahr and an anonymous reviewer for their constructive criticism. MG also wants to thank Brett Gladman for his helpful comments and suggestions.

Editorial Handling—Dr. Andy Rivkin

REFERENCES

Bowell E., Wasserman L. H., Muinonen K., and McNaught R. H. 1993. A search for the lost asteroid (719) Albert (abstract). *Bulletin of the American Astronomical Society* 25:1118.

Danby J. M. A. 1992. *Fundamentals of celestial mechanics*, 2 ed. Richmond, Virginia: Willman-Bell, Inc.

Decyk V. K., Norton C. D., and Szymanski B. K. 1997. Introduction to object-oriented concepts using Fortran90. http://exodus.physics.ucla.edu/Fortran95/. Accessed December 31, 2009.

Gladman B., Kavelaars J., Petit J.-M., Ashby M. L. N., Parker J., Coffey J., Jones R. L., Rousselot P., and Mousis O. 2009. Discovery of the first retrograde transneptunian object. *The Astrophysical Journal* 697:L91–L94.

Granvik M. and Muinonen K. 2005. Asteroid identification at discovery. *Icarus* 179(1):109–127.

Granvik M. and Muinonen K. 2008. Asteroid identification over apparitions. *Icarus* 198(1):130–137.

Granvik M., Virtanen J., Muinonen K., Bowell E., Koehn B., and Tancredi G. 2003. Transneptunian object ephemeris service (TNOEPH). *Earth, Moon and Planets* 92:73–78.

Jeffreys H. 1946. An invariant form for the prior probability in estimation problems. *Proceedings of the Royal Society of London Series A* 186:453–461.

Lehtinen M. S. 1988. On statistical inversion theory. In *Theory and applications of inverse problems*, edited by Haario H. Pitman Research Notes in Mathematics Series, vol. 167. Harlow, UK: Longman Scientific and Technical. pp. 46–57.

Milani A. 1999. The asteroid identification problem I. Recovery of lost asteroids. *Icarus* 137(2):269–292.

Milani A., Denneau L., Pierfederici F., and Jedicke R. 2007. Data Exchange Standard (2.02) for solar system object detections and orbits A tool for Input/Output definition and control, Technical Report Pan-STARRS Document Control 530-004-02. Institute for Astronomy, University of Hawai'i, USA.

Muinonen K. 1996. Orbital covariance eigenproblem for asteroids and comets. *Monthly Notices of the Royal Astronomical Society* 280:1235–1238.

Muinonen K. and Bowell E. 1993. Asteroid orbit determination using Bayesian probabilities. *Icarus* 104(2):255–279.

Muinonen K., Virtanen J., and Bowell E. 2001. Collision probability for Earth-crossing asteroids using orbital ranging. *Celestial Mechanics and Dynamical Astronomy* 81(1–2):93–101.

Oszkiewicz D. A., Muinonen K., Virtanen J., and Granvik M. 2009.

Asteroid orbital ranging using Markov-Chain Monte Carlo. *Meteoritics & Planetary Science* 44. This issue.

Virtanen J. 2005. Asteroid orbital inversion using statistical methods, Ph.D. thesis, Department of Astronomy, Faculty of Science, University of Helsinki, Finland.

Virtanen J. and Muinonen K. 2006. Time evolution of orbital uncertainties at discovery for the impactor candidate 2004 AS. *Icarus* 184(2):289–301.

Virtanen J., Muinonen K., and Bowell E. 2001. Statistical ranging of asteroid orbits. *Icarus* 154(2):412–431.

Virtanen J., Muinonen K., and Mignard F. 2005. Asteroid orbits with Gaia: simulated examples. In *Three-dimensional universe with Gaia*, edited by Perryman M. Special Publications SP-576. Noordwijk: European Space Agency. pp. 325–328.

Virtanen J., Tancredi G., Bernstein G. M., Spahr T., and Muinonen K. 2008. *The solar system beyond Neptune.* Chapter "Transneptunian Orbit Computation." Tucson: The University of Arizona Press. pp. 25–40.

Virtanen J., Tancredi G., Muinonen K., and Bowell E. 2003. Orbit computation for transneptunian objects. *Icarus* 161(2):419–430.